Spatially dependent Lamb shift in a waveguide and its influence on the optical polyatomic cooperative effects

A. S. Kuraptsev [*] and I. M. Sokolov [†]
Peter the Great St. Petersburg Polytechnic University, 195251 St. Petersburg, Russia

(Received 9 January 2023; revised 27 February 2023; accepted 3 April 2023; published 13 April 2023)

We show that the Lamb shift can significantly affect the nature of the interatomic dipole-dipole interaction in structured reservoirs. The effect is explained by the difference in the Lamb shift for atoms located at different positions due to the inhomogeneity of the spatial structure of the modes of the electromagnetic field. Based on the model system involving two atoms in a waveguide, we demonstrate that this difference can be the same order as the natural linewidth of the atomic transition.

DOI: 10.1103/PhysRevA.107.042808

I. INTRODUCTION

The study of collective optical effects in atomic ensembles represents one of the most promising fields in quantum physics. It has found a number of applications in quantum metrology, frequency standardization, and quantum information science. Nowadays, it is understood that a correct theoretical description of cooperative effects keeping all the interatomic correlations requires a microscopic approach.

In the frame of microscopy, the electromagnetic dipole-dipole interaction between atoms can be interpreted as an exchange of photons, including virtual ones. A similar mechanism produces the natural linewidth of atomic transitions. Therefore, quantum optics approaches allow us to describe both spontaneous decay of individual atoms and interatomic dipole-dipole interactions within a single formalism [1–5]. However, there is one long-standing problem that is usually concealed in these approaches: the problem of the Lamb shift. In the framework of standard nonrelativistic approaches, it undergoes ultraviolet divergence. In the case of atomic ensembles in free space, one manages to bypass this problem easily; since the Lamb shift of all the atoms is the same, it can be additively included in the transition frequency [6]. However, this simple trick does not work when we deal with atomic ensembles coupled to a cavity or waveguide. In this case, the atoms located at different positions undergo different Lamb shifts due to spatial inhomogeneity of the modes of the electromagnetic field in a cavity and/or waveguide [7–11]. In turn, it can affect the interatomic dipole-dipole interaction and associated cooperative effects.

In this paper we report the investigation of the Lamb shift which depends on the position of an atom in a waveguide. On this basis, we analyze how it modifies the character of the dipole-dipole interaction. Our results demonstrate that the difference in the Lamb shift for two atoms located at different points can be comparable to the natural linewidth of the atomic transition or even exceed it. Therefore, the collective dynamics of an atomic system can be significantly affected by the Lamb shift.

II. COOPERATIVITY

According to the general quantum microscopic approach, the evolution of an ensemble which contains N atoms under the condition of a strong dipole-dipole interaction is described by the coupled dipole model [6,12–27]. In the framework of this formalism, the dynamics of the atomic-field system can be treated on the basis of the non-steady-state Schrödinger equation for the wave function of the joint system, which consists of the atoms and the electromagnetic field, including a vacuum reservoir. The Hamiltonian of this system can be represented as $\hat{H} = \hat{H}_0 + \hat{V}$, where $\hat{H}_0$ corresponds to noninteracting atoms and the electromagnetic field in an empty space and $\hat{V}$ is the interaction between the atoms and the field. The operator of the interaction $\hat{V}$ can be written in the form

$$\hat{V} = -\frac{e}{mc}\sum_{i=1}^{N} \hat{\mathbf{p}}_i \cdot \hat{\mathbf{A}}(\mathbf{r}_i), \tag{1}$$

where e is the electron charge, m is its mass, c is the speed of light in vacuum, $\hat{\mathbf{p}}_i$ is the electron momentum operator of the atom i, $\hat{\mathbf{A}}(\mathbf{r})$ is the operator of the vector potential of the electromagnetic field, and $\mathbf{r}_i$ is the position of the atom i. Considering the electric dipole atomic transitions, hereafter we assume the relation between matrix elements of the operator $\hat{\mathbf{p}}$ and the dipole momentum of transition, $\langle g|\hat{\mathbf{p}}|e\rangle = (-im\omega_0/e)\langle g|\hat{\mathbf{d}}|e\rangle$. Here $\langle g|$ and $|e\rangle$ denote the ground and excited atomic states, respectively, ω_0 is the resonant transition frequency, and i is the imaginary unit. Actually, the approximation performed together with neglecting the term proportional to $\hat{\mathbf{A}}^2$ in the operator of the interaction essentially constitutes the dipole approximation used in Ref. [6].

Formally solving the Schrodinger equation for the joint system, which consists of N atoms and the electromagnetic field, and restricting ourselves to the states containing no more than one photon (i.e., neglecting nonlinear effects), we obtain

[*] aleksej-kurapcev@yandex.ru
[†] sokolov_im@spbstu.ru

a system of equations for the amplitudes b_e of onefold atomic excited states with the coupling between atoms caused by the dipole-dipole interaction. In the Fourier representation, the set of coupled dipole equations reads (at greater length see [6])

$$\sum_{e'}[(\omega-\omega_0)\delta_{ee'}-\Sigma_{ee'}(\omega)]b_{e'}(\omega)=i\delta_{es}. \tag{2}$$

The index s as well as the indices e and e' contain information about both the number of concrete atom and the specific atomic sublevel excited in the corresponding state. The set of equations in the form represented by Eq. (2) is obtained under the assumption that at the initial time only one atom is at the excited state s; all other atoms are in their ground states and the electromagnetic field is in the vacuum state.

This method was successfully used by our group for the analysis of the optical properties of dense atomic ensembles as well as for studying light scattering from such ensembles [28–34]. Further, it allowed us to describe cooperative effects in atomic ensembles located in a Fabry-Pérot cavity [35,36], near a single conducting surface [37–39], and in a waveguide [40,41]. Very similar approaches were used by other groups [42–45], in particular, in application to photonic crystals [9,46–50].

The matrix $\Sigma_{ee'}(\omega)$ is a key quantity in the theory. It describes both spontaneous decay and photon exchange between the atoms. The general equation for this matrix is

$$\Sigma_{ee'}(\omega)=\sum_{g}V_{e;g}V_{g;e'}\zeta(\hbar\omega-E_g)+\sum_{ee}V_{e;ee}V_{ee;e'}\zeta(\hbar\omega-E_{ee}). \tag{3}$$

This equation includes matrix elements of the operator $\hat{V}$ of the interaction between atoms and the electromagnetic field and $\zeta(x)$ is a singular function given by the relation $\zeta(x)=-i\pi\delta(x)+P(1/x)$, where P denotes the principal value. To calculate the matrix $\Sigma_{ee'}(\omega)$ in Eq. (3), we should perform a summation over resonant single-photon states g (when all the atoms are in their ground states) as well as over nonresonant states with two excited atoms and one photon ee (for details see [6]).

When we want to describe cooperative effects which occur in atomic ensembles located in a waveguide, we should use the field operator $\hat{\mathbf{A}}(\mathbf{r})$ corresponding to the inner space inside a waveguide. In the case of perfectly conducting waveguide with a rectangular cross section, $\hat{\mathbf{A}}(\mathbf{r})$ reads

$$\hat{\mathbf{A}}(\mathbf{r})=\sum_{\mathbf{k},\alpha}\sqrt{\frac{\hbar}{2\omega_k}}\mathbf{A}_{\mathbf{k},\alpha}(x,y)\times\exp(ik_zz)\hat{a}_{\mathbf{k},\alpha}+\text{H.c.}, \tag{4}$$

where α denotes the type of waveguide mode (TE or TM), $\hat{a}_{\mathbf{k},\alpha}$ is the operator of annihilation of a photon in the corresponding

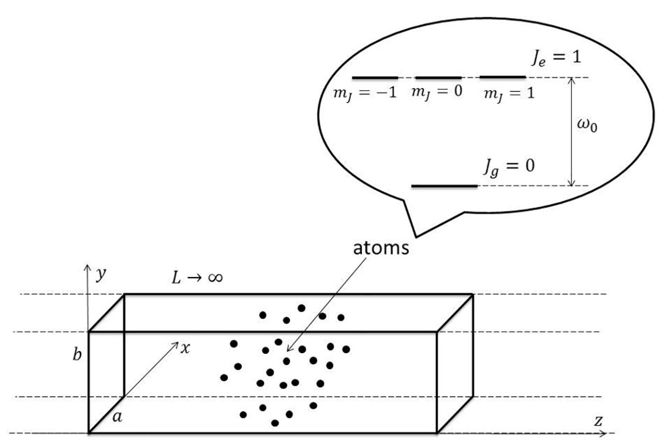

FIG. 1. Sketch of the waveguide and the atomic ensemble inside it. The inset shows the model structure of atomic levels used in the study of cooperativity. Here a and b are the dimensions of a rectangular cross section of a waveguide, L is its length (infinite), J_g is the total angular momentum of an atom in the ground state, J_e is its value in the excited state, m_J is the projection of the total angular momentum on the quantization axis z, and ω_0 is the transition frequency.

mode, ω_k is the photon frequency,

$$A^x_{\mathbf{k},\mathrm{TE}}(x,y)=-\frac{k_n}{k_m^2+k_n^2}\times B_{mn}\cos(k_mx)\sin(k_ny), \tag{5}$$

$$A^y_{\mathbf{k},\mathrm{TE}}(x,y)=\frac{k_m}{k_m^2+k_n^2}\times B_{mn}\sin(k_mx)\cos(k_ny), \tag{6}$$

$$A^z_{\mathbf{k},\mathrm{TE}}(x,y)\equiv 0, \tag{7}$$

$$A^x_{\mathbf{k},\mathrm{TM}}(x,y)=\frac{k_zk_m}{k\left(k_m^2+k_n^2\right)}\times B_{mn}\cos(k_mx)\sin(k_ny), \tag{8}$$

$$A^y_{\mathbf{k},\mathrm{TM}}(x,y)=\frac{k_zk_n}{k\left(k_m^2+k_n^2\right)}\times B_{mn}\sin(k_mx)\cos(k_ny), \tag{9}$$

$$A^z_{\mathbf{k},\mathrm{TM}}(x,y)=-\frac{i}{k}B_{mn}\sin(k_mx)\sin(k_ny). \tag{10}$$

Here $k_m=m\pi/a$, $k_n=n\pi/b$, and $k=\sqrt{k_m^2+k_n^2+k_z^2}=\omega_k/c$. The indices m and n are positive integers for TM modes; for TE modes $m,n=0,1,2,\ldots$, but both indices cannot be zero together. In addition, B_{mn} is the normalization constant, which can be obtained on the basis of the standard form of the field Hamiltonian. A reference point is chosen at one of the corners of the cross section, so the space in a waveguide corresponds to the positive values of the coordinates x and y, as shown in Fig. 1.

As we assume an infinite length of a waveguide, the sum over the field states in Eq. (3) should be calculated in the limit of infinite length of the quantization volume along the z axis, $L_q \to \infty$. This implies summation over the types of field modes in a waveguide (TE and TM), summation over the transverse indices m and n, and the integration over a continuous variable k_z (see [40] for detail):

$$\sum_g \text{ or} \sum_{ee} \to \frac{L_q}{2\pi} \sum_{\text{TE,TM}} \sum_{m,n} \int_{-\infty}^{+\infty} dk_z.$$

The number of equations in the system (2) is determined by the quantity of states where only one atom in the ensemble is excited at the specific sublevel e whereas all other atoms are in their ground states. So the size of the matrix $\Sigma_{ee'}(\omega)$ depends on the number of atoms N and the structure of the atomic levels. If the ground state is degenerate, the number of equations increases with an increase of N extremely fast (at least exponentially). Therefore, in microscopy, one usually exploits model schemes of levels, such as the so-called V scheme: The ground state $|g_i\rangle$ of an isolated atom i is nondegenerate with the total angular momentum $J_g = 0$, whereas the excited states $|e_i\rangle$ is threefold degenerate with $J_e = 1$ and natural free space linewidth γ_0 (see the inset in Fig. 1). The three degenerate substates $|e_{i,m_J}\rangle$ correspond to the three possible projections $m_J = 0, \pm 1$ of the total angular momentum $\mathbf{J}_e$ on the quantization axis z. The resonant frequency ω_0 of atoms defines the natural length scale $1/k_0 = c/\omega_0$. In the framework of this model, the number of equations is $3N$.

Actually, the approach employed allows us to describe both monatomic dynamics and cooperative effects caused by interatomic dipole-dipole interactions from a single position. In the case when the indices e and e' refer to different atoms, the matrix element $\Sigma_{ee'}(\omega)$ describes the dipole-dipole interaction. In the case when the states e and e' refer to the same atom, the imaginary part of $\Sigma_{ee'}(\omega)$ describes the spontaneous decay rate of a given excited state, whereas the real part of $\Sigma_{ee'}(\omega)$ is divergent. In its physical sense, the latter represents the Lamb shift of the atomic transition frequency.

III. LAMB SHIFT

Since the Lamb shift of the given atomic level is caused by the emission and absorbtion of virtual photons which couple this level with all other levels (including the continuous spectrum of electronic states), we can no longer use the model scheme of levels. When calculating the Lamb shift, we have to consider a real atom, taking into account all the electronic states. Thus, disclosing the real part of the corresponding matrix element in Eq. (3), the Lamb shift of the energy level n' reads

$$\Delta E_{n'} = \sum_{m'} \sum_{\mathbf{k},\alpha} \frac{|\langle m', 1_{\mathbf{k},\alpha}|\hat{V}|n', \text{vac}\rangle|^2}{E_{n'} - E_{m'} - \hbar\omega_k}. \tag{11}$$

Here the index m' indicates the electronic state (including both bonded states with a discrete energy spectrum and ionized states with a continuous spectrum) and $1_{\mathbf{k},\alpha}$ means that there is one photon in the corresponding mode. Equation (11) naturally coincides with a well-known formula from standard textbooks (see, for example, Ref. [51]).

Exact calculation of the sum over field states in Eq. (11) gives us linear divergence with the photon energy. It is explained by the fact that Eq. (11) contains the electromagnetic energy of a free electron, which is also divergent. According to Bethe's approach [52], we should perform the renormalization procedure, i.e., subtracting the electromagnetic energy of a free electron from Eq. (11). Thus, the observable value of the Lamb shift is $\Delta E_{n'}^{\text{obs}} = \Delta E_{n'} - \Delta E_{n'}^{\text{free}}$, where $\Delta E_{n'}^{\text{free}}$ is the value of $\Delta E_{n'}$ when the frequencies of all the transitions approach zero $E_{n'} - E_{m'} \to 0$. The renormalization should reduce the character of the ultraviolet divergence down to the logarithmic one.

In order to calculate the sum over the intermediate electron states $|m'\rangle$ in Eq. (11), we should specify the kind of atom. In this paper we consider a hydrogen atom and focus our attention on the $1s \leftrightarrow 2p$ transition. It is known that in the first approximation, p states do not undergo a Lamb shift [52,53]. Therefore, the shift of the transition frequency is determined by the Lamb shift of the ground state $1s$.

The Lamb shift of the $1s$ state of a hydrogen atom remains weakly divergent after renormalization. Following Bethe [52], we should introduce the cutoff energy of a photon E_c and take into account in Eq. (11) only the photons having an energy less than E_c. Our numerical simulation has proved that the asymptote of the function $\Delta E_{n'}^{\text{obs}}(E_c)$ is indeed logarithmic, $\Delta E_{n'}^{\text{obs}}(E_c) = E_1 \ln(E_c/E_2)$. Actually, it is the analog of Bethe's logarithm; the parameters E_1 and E_2 can be found using the least-mean-square method. Finally, the cutoff energy should be taken as $E_c = mc^2$.

Our numerical simulation has shown that all the hyperfine and Zeeman sublevels of the $1s$ state of the hydrogen atom in a waveguide undergo the same Lamb shift. Figure 2 shows this Lamb shift depending on the position of an atom (x_1, y_1). In Fig. 2(a) the dimensions of the waveguide are $a = 4$ and $b = 2$ (hereafter we consider the inverse wave number of radiation resonant to the atomic transition $k_0^{-1} = c/\omega_0$ as a unit of length), which correspond to a single-mode waveguide with respect to the $1s \leftrightarrow 2p$ transition. Here we see that a Lamb shift reaches its maximum when the atom is located at the center of the cross section of a waveguide. Towards the walls, the value of the Lamb shift decreases. The slope of the x dependence of the Lamb shift is small in the central area, whereas near the edges it becomes very large. When the atom approaches the wall, the Lamb shift approaches some asymptotic value. Our numerical simulation shows that, in the case $y_1 = b/2$, for example, this asymptote is 5370 MHz for the dimensions $a = 4$ and $b = 2$.

With increasing transverse dimensions of a waveguide a and b, coordinate dependence of the Lamb shift flattens. In Fig. 2(b) we show this dependence for the case $a = b = 5$. This corresponds to a multimode waveguide with respect to the $1s \leftrightarrow 2p$ transition. Four modes are allowed: TE_{10}, TE_{01}, TE_{11}, and TM_{11}. The flattening of the coordinate dependence in the central area is explained by the increasing number of field modes with increasing transverse dimensions. For large values of a and b, the Lamb shift of an atom located in the central area of a waveguide naturally resembles its free-space value.

In Fig. 2 we can see that the spread in the Lamb shift is hundreds of megahertz, which is comparable to the natural linewidth of a hydrogen $2p \to 1s$ transition, $\gamma_0 = 100$ MHz. Therefore, the spatial dependence of the Lamb shift can affect

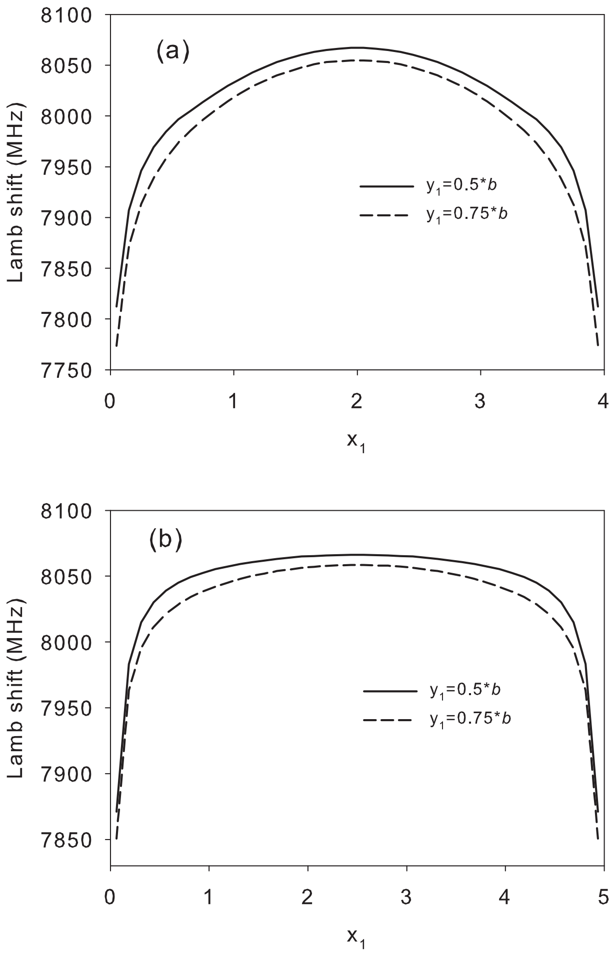

FIG. 2. Lamb shift of the 1s state of a hydrogen atom depending on its position in a waveguide. The dimensions of the cross section of a waveguide are (a) $a = 4$ and $b = 2$ and (b) $a = b = 5$.

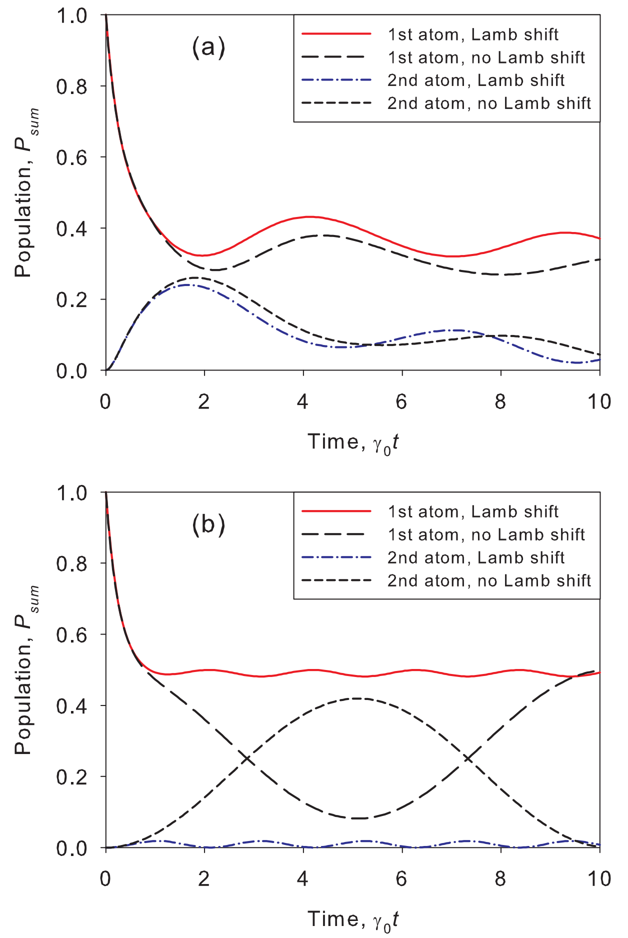

FIG. 3. Dynamics of the excited-state population. Here $a = 4$ and $b = 2$. The position of the first atom (initially excited) is at $x_1 = 2.05$ and $y_1 = 1$. The position of the second atom (initially unexcited) is at $y_2 = 1.5$ and (a) $x_2 = 3.05$ and (b) $x_2 = 3.95$.

the character of the dipole-dipole interaction between different atoms in a waveguide. This inference is confirmed by Fig. 3.

In Fig. 3 we analyze two equal atoms located in a waveguide and coupled by the dipole-dipole interaction. Here we use the model scheme of levels mentioned previously when discussing cooperativity and shown in the inset in Fig. 1. Here we hold the realistic ratio between Lamb shifts and a natural linewidth. Since the Lamb shift is a single-atom effect, we are able to merely include the single-atom Lamb shift in the coupled dipole equations (2) that describe the excitation dynamics of the two atoms. The first atom is considered to be initially excited and the populated Zeeman sublevel of the excited state is $m_J = -1$. The second atom is initially unexcited. Figure 3 shows the dynamics of the total excited-state population P_{sum} calculated as the sum of populations over all the Zeeman sublevels, separately for the first and second atoms. Here we compare the case when the Lamb shift is taken into account with the case when it is not.

One can clearly see that accounting for Lamb shifts affects the behavior of the atomic excited-state populations. Figure 3(a) refers to the case when the difference in Lamb shift for the first atom and for the second one is approximately $0.5\gamma_0$. Here the effect is not dramatic but is already observable. Figure 3(b) corresponds to such an arrangement of atoms that the difference in Lamb shift is almost $3\gamma_0$. Here the effect is significant. Such a difference in Lamb shift makes atoms almost nonresonant with each other. Therefore, when Lamb shifts are taken into account, the atoms exhibit behavior similar to independent ones [40], while originally it is two resonant and closely spaced atoms that should be strongly coupled and exhibit cooperative behavior.

Quasiperiodic oscillations observed in Fig. 3 are connected with the energy exchange between the atoms. We can see that the Lamb shift alters these oscillations. It is particularly manifested in Fig. 3(b). A qualitative explanation of the observed behavior of curves is as follows. Accounting for the Lamb shift, almost nonresonant atoms evolve close to independent ones. So the corresponding curves (the first and third) almost reproduce the single-atom case: The first curve demonstrates incomplete spontaneous decay in a single-mode waveguide [40] and the third curve is close to zero. The weak dipole-dipole interaction between atoms leads to small oscillations caused by a photon exchange. In the case, when we do not take into account the Lamb shift, we deal with two resonant atoms strongly coupled with each other. Such a dimer has its own unique collective states with lifetimes which significantly differ from the natural lifetime of the excited states of a free atom. These collective lifetimes determine the period of oscillations and its specific value depends on the specific arrangement of both atoms.

ACKNOWLEDGMENTS

This work was supported by the Russian Science Foundation (Grant No. 21-72-10004). The results of the work were obtained using computational resources of Peter the Great St. Petersburg Polytechnic University Supercomputer Center.

[1] M. J. Stephen, J. Chem. Phys. **40**, 669 (1964).
[2] D. A. Hutchinson and H. F. Hameka, J. Chem. Phys. **41**, 2006 (1964).
[3] R. Bonifacio, P. Schwendimann, and F. Haake, Phys. Rev. A **4**, 302 (1971).
[4] R. Bonifacio, P. Schwendimann, and F. Haake, Phys. Rev. A **4**, 854 (1971).
[5] Z. Ficek, R. Tanas, and S. Kielich, Opt. Acta **33**, 1149 (1986).
[6] I. M. Sokolov, D. V. Kupriyanov, and M. D. Havey, J. Exp. Theor. Phys. **112**, 246 (2011).
[7] A. A. Belov, Yu. E. Lozovik, and V. L. Pokrovskii, Zh. Eksp. Teor. Fiz. **96**, 552 (1989) [Sov. Phys. JETP **69**, 312 (1989)].
[8] P. Horak, P. Domokos, and H. Ritsch, Europhys. Lett. **61**, 459 (2003).
[9] X.-H. Wang, Y. S. Kivshar, and B.-Y. Gu, Phys. Rev. Lett. **93**, 073901 (2004).
[10] P. Yao, C. Van Vlack, A. Reza, M. Patterson, M. M. Dignam, and S. Hughes, Phys. Rev. B **80**, 195106 (2009).
[11] M. V. Rybin, S. F. Mingaleev, M. F. Limonov, and Y. S. Kivshar, Sci. Rep. **6**, 20599 (2016).
[12] O. Morice, Y. Castin, and J. Dalibard, Phys. Rev. A **51**, 3896 (1995).
[13] J. Ruostekoski and J. Javanainen, Phys. Rev. A **55**, 513 (1997).
[14] S. Balik, A. L. Win, M. D. Havey, I. M. Sokolov, and D. V. Kupriyanov, Phys. Rev. A **87**, 053817 (2013).
[15] J. Pellegrino, R. Bourgain, S. Jennewein, Y. R. P. Sortais, A. Browaeys, S. D. Jenkins, and J. Ruostekoski, Phys. Rev. Lett. **113**, 133602 (2014).
[16] S. L. Bromley, B. Zhu, M. Bishof, X. Zhang, T. Bothwell, J. Schachenmayer, T. L. Nicholson, R. Kaiser, S. F. Yelin, M. D. Lukin, A. M. Rey, and J. Ye, Nat. Commun. **7**, 11039 (2016).
[17] W. Guerin, M. O. Araujo, and R. Kaiser, Phys. Rev. Lett. **116**, 083601 (2016).
[18] R. Röhlsberger, K. Schlage, B. Sahoo, S. Couet, and R. Ruffer, Science **328**, 1248 (2010).
[19] J. D. Pritchard, D. Maxwell, A. Gauguet, K. J. Weatherill, M. P. A. Jones, and C. S. Adams, Phys. Rev. Lett. **105**, 193603 (2010).
[20] J. Keaveney, A. Sargsyan, U. Krohn, I. G. Hughes, D. Sarkisyan, and C. S. Adams, Phys. Rev. Lett. **108**, 173601 (2012).
[21] L. Weller, R. J. Bettles, P. Siddons, C. S. Adams, and I. G. Hughes, J. Phys. B **44**, 195006 (2011).
[22] R. Friedberg and J. T. Manassah, Phys. Rev. A **84**, 023839 (2011).
[23] D. V. Kuznetsov, K. Roerich, and M. G. Gladush, J. Exp. Theor. Phys. **113**, 647 (2011).
[24] M. O. Scully, Phys. Rev. Lett. **115**, 243602 (2015).
[25] A. S. Kuraptsev and I. M. Sokolov, Phys. Rev. A **90**, 012511 (2014).
[26] C. C. Kwong, T. Yang, M. S. Pramod, K. Pandey, D. Delande, R. Pierrat, and D. Wilkowski, Phys. Rev. Lett. **113**, 223601 (2014).
[27] C. C. Kwong, D. Wilkowski, D. Delande, and R. Pierrat, Phys. Rev. A **99**, 043806 (2019).
[28] Y. A. Fofanov, A. S. Kuraptsev, I. M. Sokolov, and M. D. Havey, Phys. Rev. A **84**, 053811 (2011).
[29] I. M. Sokolov, A. S. Kuraptsev, D. V. Kupriyanov, M. D. Havey, and S. Balik, J. Mod. Opt. **60**, 50 (2013).
[30] A. S. Kuraptsev and I. M. Sokolov, Phys. Rev. A **91**, 053822 (2015).
[31] S. Roof, K. Kemp, M. Havey, I. M. Sokolov, and D. V. Kupriyanov, Opt. Lett. **40**, 1137 (2015).
[32] S. E. Skipetrov, I. M. Sokolov, and M. D. Havey, Phys. Rev. A **94**, 013825 (2016).
[33] A. S. Kuraptsev and I. M. Sokolov, Laser Phys. **27**, 115201 (2017).
[34] A. S. Kuraptsev, I. M. Sokolov, and M. D. Havey, Phys. Rev. A **96**, 023830 (2017).
[35] A. S. Kuraptsev and I. M. Sokolov, J. Exp. Theor. Phys. **123**, 237 (2016).
[36] A. S. Kuraptsev and I. M. Sokolov, Phys. Rev. A **94**, 022511 (2016).
[37] A. S. Kuraptsev and I. M. Sokolov, J. Exp. Theor. Phys. **127**, 455 (2018).
[38] A. S. Kuraptsev and I. M. Sokolov, Laser Phys. **28**, 085203 (2018).
[39] A. S. Kuraptsev and I. M. Sokolov, Phys. Rev. A **100**, 063836 (2019).
[40] A. S. Kuraptsev and I. M. Sokolov, Phys. Rev. A **101**, 053852 (2020).
[41] A. S. Kuraptsev and I. M. Sokolov, Phys. Rev. A **105**, 063513 (2022).
[42] E. Shahmoon and G. Kurizki, Phys. Rev. A **87**, 033831 (2013).
[43] A. M. Mahmoud, I. Liberal, and N. Engheta, Opt. Mater. Express **7**, 415 (2017).
[44] G. Fiscelli, L. Rizzuto, and R. Passante, Phys. Rev. A **98**, 013849 (2018).
[45] Y. Jiang, J. Phys. Commun. **2**, 055002 (2018).
[46] S. Y. Xie and Y. P. Yang, Eur. Phys. J. D **42**, 163 (2007).
[47] Q. Liu, H. Song, W. Wang, X. Bai, Y. Wang, B. Dong, L. Xu, and W. Han, Opt. Lett. **35**, 2898 (2010).
[48] X.-S. Huang, H.-L. Liu, D. Wang, X.-T. Mo, and H.-T. Liu, Sci. China Phys. Mech. Astron. **56**, 524 (2013).

[49] J. S. Douglas, H. Habibian, C.-L. Hung, A. V. Gorshkov, H. J. Kimble, and D. E. Chang, Nat. Photon. **9**, 326 (2015).

[50] E. Munro, L. C. Kwek, and D. E. Chang, New J. Phys. **19**, 083018 (2017).

[51] P. W. Milonni, *The Quantum Vacuum: An Introduction to Quantum Electrodynamics* (Academic, San Diego, 1994).

[52] H. A. Bethe, Phys. Rev. **72**, 339 (1947).

[53] H. A. Bethe and E. E. Salpeter, *Quantum Mechanics of One- and Two-Electron Atoms* (Springer, Berlin, 1957).